Spatio-Temporal Pattern Recognition of Dendritic Spines and Protein Dynamics Using Live Multichannel Fluorescence Microscopy

Vincent On[1], Atena Zahedi[2], Iryna Ethell[3] and, Bir Bhanu[1,2]

[1]Department of Electrical and Computer Engineering, University of California, Riverside, CA 92521, USA

[2] Department of Bioengineering, University of California, Riverside, CA 92521, USA

[3]Department of Biomedical Sciences, University of California, Riverside, CA 92521, USA

Email: von001@ucr.edu, azahe001@ucr.edu, iryna,ethell@ucr.edu, bhanu@cris.ucr.edu

Abstract—Actin-regulating proteins, such as cofilin, are essential in regulating the shape of dendritic spines, and synaptic plasticity in both neuronal functionality as well as in neurodegeneration related to aging. The analysis of the motility of cofilin in fluorescence video-microscopy allows the discovery of its effects on cell functions. However, the flow of cofilin has not been analyzed to date by automatic means. This paper presents a novel automated pattern recognition system to analyze protein trafficking in neurons. Using spatio-temporal information present in multichannel fluorescence videos, the system generates a temporal maximum intensity projection that enhances the signal-to-noise ratio of important biological structures, segments and tracks dendritic spines, and quantifies the flux and density of proteins in spines. The temporal dynamics of spines is used to generate spine energy images which are used to automatically classify the shape of dendritic spines as stubby, mushroom, or thin. By tracking these spines over time and using their intensity profiles, the system is able to analyze the flux patterns of cofilin and other fluorescently stained proteins. The cofilin flux patterns is found to be correlated with the dynamically changing dendritic spine shapes. The results are presented using multichannel fluorescence videos.

Keywords—dendritic spines; protein flux; classification; multichannel imaging;

I. INTRODUCTION

Cofilin is an actin-severing protein that exists in specialized locations within cells and it directly correlates with their function [1], [2]. Each cell compartment can be defined by its own structural and chemical composition. The localization of proteins can provide information about the protein's activity, associated transduction pathways, and interactions with other proteins. Understanding of subcellular changes in their localization over time is critical in studying their function. In this paper, we investigate role of the actin-severing protein, cofilin, in regulating the remodeling of spines. Dendritic spines are small protrusions located on the surface of neuronal dendrites. These dendritic spines contain the post-synaptic sites of excitatory synapses in the central nervous system (CNS) [3]–[7]. The various shapes of dendritic spines can have a strong impact on the development of cognitive disabilities and neurological diseases. Cofilin's role in remodeling dendritic spines is to sever and disassemble the actin cytoskeleton that provides the structure to dendritic spines. Elevated levels of cofilin have previously been shown to contribute to loss of synapses and spines in neurodegenerative disorders, such as Alzheimer's disease (AD) [8], [9]. However, the precise mechanism underlying cofilin-mediated loss of synapses is unclear. Therefore, it is important to quantify the motility of cofilin and examine how the localization of cofilin affects dendritic spine shape.

Many previous studies involving the effects of proteins on synaptic remodeling have primarily used manual examination, segmentation, and classification. Most of these biological studies have used simple user-operated software such as *imageJ* to manually segment regions of interest (ROIs). Other studies have used visualization systems such as Imaris or Neurolucida [10]. However, both of these systems require z-stack information and are highly dependent on parameter selection. These manual methods can be a tedious and time consuming process, and is prone to user bias, especially when analyzing time-lapse videos. Hence, it is advantageous to develop image processing algorithms to automatically segment ROIs and extract features for the analysis of live fluorescence videos.

In order to automatically correlate cofilin localization with dendritic spine shapes, we must also automatically segment and analyze dendritic spines in the same image. Due to the small size of dendritic spines, it is difficult to acquire images with sufficient resolution and contrast to properly analyze the dynamic structures. Many experiments compensate for this by analyzing the maximum intensity projection of a z-stack. Capturing these z-stacks would be disadvantageous for us as we are already capturing two separate fluorescence channels; a green channel which was stained with wild type (wt)-Cofilin-GFP to label cofilin proteins and a red channel stained with TdTomato to provide accurate spine structural information. In addition, in order to analyze the spatio-temporal relationship between dendritic spines and cofilin, a time series of sufficient temporal resolution must be captured. To improve our signal-to-noise ratio, we present a method that uses the spatio-temporal information of the time series of video to enhance each frame of the video without the need to acquire z-stack data.

In this paper, we propose a novel automated pattern recognition system that analyzes protein trafficking in neurons using multi-channel florescence microscopy and

correlates back to spine shape/function. Unlike previous work, our proposed method uses video bioinformatics algorithms to obtain systematic, spatio-temporal pattern information on cofilin dynamics. The system is used specifically to examine cofilin's effect on the shape and motion of dendritic spines. Fluorescence microscopy is used because the intensity level of pixels are assumed to be proportional to the amount of stained proteins in the image. Due to cofilin's small size, which is at the subpixel level, individual proteins cannot be tracked. However, our system is able to estimate the change of cofilin density in the dendritic spines by measuring their intensity levels. We also use a spine energy representation similar to an existing motion pattern representation called gait energy image (GEI) to capture spine motion in a single image so as to extract useful features that can be used to classify segmented spine shapes. By correlating the extracted spine shape with the observed cofilin transport dynamics, we can analyze and gain insights into the underlying biological processes.

II. RELATED WORK

To the best of our knowledge, cofilin has never been automatically quantified. Previously, another actin-regulating protein paxillin, has been automatically analyzed in non-neuronal florescence images [11]. However, only paxillin dense regions that are above a threshold are tracked. These paxillin dense regions are also sparse and appear much brighter than the rest of the cell. However, this is not the case for cofilin located in dendrites and dendritic spines as it is more uniformly distributed. Also cofilin dense regions may disperse and form over time, making tracking these clusters impossible. Bosch et al. [12] have manually studied the effect of cofilin on the remodeling of dendritic spine substructures. This paper classified cofilin transport in dendritic into four different patterns: persistent increase in concentration, transient increase, transient decrease, and persistent decrease. Using this information, they found that the type of cofilin transport correlated with the remodeling of dendritic spine shapes.

There are some existing methods that automatically examine the flow of proteins in cells. Many of these methods estimate individual particle trajectories over time by using frame by frame object detection [13] and associating the objects across time. An issue with these methods is that they do not perform well with high particle density and in the presence of noise. Another approach is to partition the cell into regions and estimate particle flux by the intensity level or protein density in the regions [14], [15]. Pecot et al. [15] developed a method that involves partitioning the cell into predefined regions of set sizes and shape. By counting the number of particles or measuring changes in the intensity levels, they were able to estimate the flux of these particles through the boundaries between regions. One limitation of this method is that the regions must be rigid and the choice of region size affects the performance. Also the experiments on live samples used micro-fabricated patterns [16] to constrain the cell shape so that the partitioned regions remained the same throughout the experiment.

To correlate cofilin transport with dendritic spine morphology, spines must be simultaneously segmented and classified. Spine segmentation methods can be divided into two groups, classification based [17] and centerline extraction based [18]–[21]. The classification methods classify individual pixels into different groups such as spine, dendrite, or background [17]. The method by Rodriguez et al. [17] uses the pixel distance to the close surface point as a feature in classification, however, this can produce spurious spine detection and is sensitive to noise. Centerline methods involve detecting the backbone of the dendrites and segmenting spines by their relationship to the backbone. Traditional methods have difficulty when the dendrite width varies along its orientation. In our system, the method [22] is used to detect a center region using gradient vector flow [23] instead of a thin backbone. This allows us to compensate for varying dendritic spine widths.

After segmenting spines, classification of shape type is advantageous in analyzing biological conditions. Basu et al. [24] uses a decision tree classifier to classify spines by using neck length, spine height, head width. An issue with these features is that since the resolution is so low, many of these features are measured in only a few pixels. This leads to an increased likelihood of measurement error and sensitivity in classification. One of the features used by our pattern recognition system is an adaption of gait energy image (GEI) [25]. GEI is a spatio-temporal gait representation that has been widely used to characterize human walking patterns. GEI has previously been shown to be highly effective for recognition of different individuals. Like GEI, we use spine energy images (SEI) to aid us in the classification of dendritic spine shapes such as mushroom, thin, and stubby. Unlike previous work SEI allows for the use of spatio-temporal information in classification.

The key contributions of our work are: a) that for the first time an automated algorithm suite is developed and used to quantify the movement of cofilin in dendrites and spines, and correlate to spine shape using multi-channel fluorescence live videos. b) We also use spatio-temporal information to enhance the signal-to-noise ratio in our videos. c) Automated analysis of multiple fluorescent probes in time-lapse videos provides a method for tracking the local distribution of cofilin while simultaneously analyzing the effects on spine shape. Understanding the dynamics of cofilin within sub-neuronal compartments is critical to understanding its function in regulating the morphological structure and functionality of synapses.

III. THE PROPOSED METHOD

The proposed method is separated into three parts: Dendritic spine segmentation, protein motility extraction and
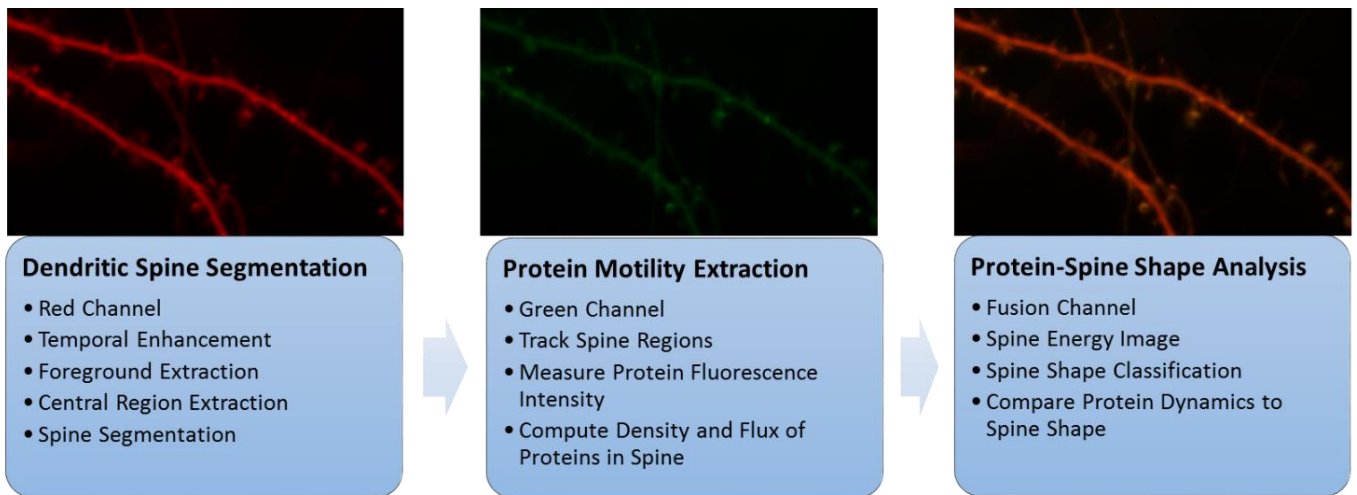
Fig. 1 System Overview Diagram. Dendritic spine segmentation subsystem uses the red fluorescence channel to extract the foreground, central region, and spines. Protein motility extraction subsystem uses green fluorescence channel to measure cofilin levels and transport in spines. Protein-spine shape analysis subsystem uses both channels and temporal information to compare spine shape and cofilin flow.

cofilin-spine shape analysis. A diagram of our workflow is shown in Fig. 1.

Dendritic Spine Segmentation

The algorithm for dendritic spine segmentation begins by estimating the foreground or region of interest in each frame. The foreground in our case is any pixel illuminated by fluorescent proteins in a dendritic structure. The algorithm starts by computing the maximum intensity projection of the time series of video frames. Given a video consisting of N_v frames, this temporal maximum intensity projection (TMIP) is defined as follows:

$$T(x, y) = \max_t I(x, y, t), \qquad (1)$$
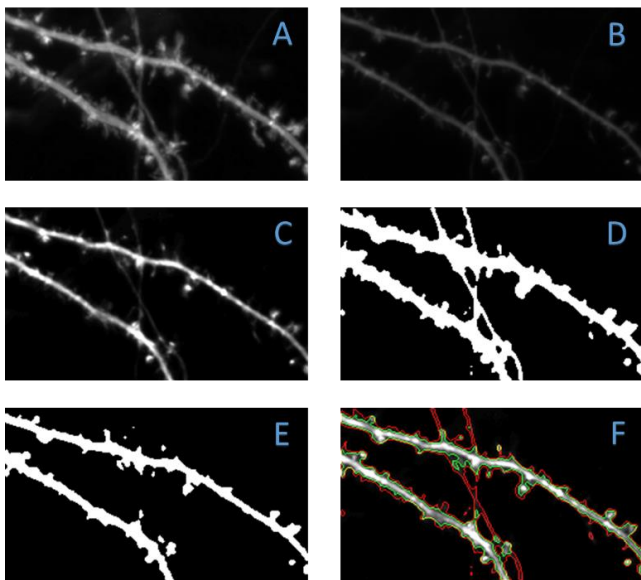
Fig. 2. A) Temporal maximum intensity projection (TMIP). B) Original frame. C) Enhanced frame. D) Extracted foreground without TMIP. E) Foreground with TMIP. F) Overlay of both foregrounds (red = without TMIP, green = with TMIP) on enhanced frame.

where $I(x,y,t)$ is the image at time t. Because we are taking the maximum intensity of a pixel along the time dimension, a TMIP pixel will be brighter if a structure strongly fluoresced at that location for any time in the video. The pixel value will be low for any background structures such as dendrites or axons outside of our focal distance. The TMIP is then max-min normalized into a filter whose values will be used as weights for enhancing the signal-to-noise ratio in the image. For every frame, the TMIP is multiplied to the image as weights. This normalization procedure is summarized in the following equation:

$$I'(x, y, t) = \frac{T(x, y) - T_{\min}}{T_{\max} - T_{\min}} * I(x, y, t). \qquad (2)$$

This allows for structures that are brighter in the TMIP to be enhanced in each frame, while background structures such as axons or dendrites outside our depth of focus to be suppressed. Because the information in the current frame is being used, no artifacts will be created from the bright regions in the TMIP. The TMIP, an original image and a temporally enhanced image are shown in Fig. 2. A rough segmentation of the dendrites and spines can now be computed by using the Otsu's method [26]. This rough segmentation is our foreground which can be used to extract the central region of the dendrite. Once the foreground is computed, the contours of the dendrites and dendritic spines can be acquired by removing all interior pixels of the ROI leaving only the outline.

After computing the foreground, we compute the central regions or backbone of the dendrites [22]. Previous methods have used a simple skeletonization procedure on the dendrite segmentation until only a thin backbone remained. The skeleton of a sample image (Fig. 3A) is shown in Fig. 3B. However, this backbone does not give the best representation of a dendrite and does not provide information such as the changing width of the dendrite. We start by acquiring a rough segmentation of the foreground using thresholding the TMIP enhanced frame by Otsu's method. Next, a modified gradient vector flow is computed, in which vectors are orientated
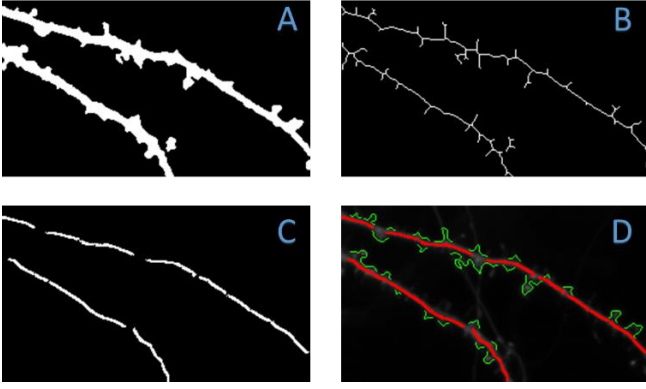
Fig. 3. A) Foreground of dendritic spines. B) Skeletonization of A. C) Central region compute from A. D) Segmented spine contours and central region overlaid to original frame.

towards the center of a structure. Starting from every edge pixel, the algorithm follows the path of vectors until it encounters a vector greater than 90 degrees from the current vector. Both these pixels will now be marked as a central dendrite pixel. Noise and possible spine central regions are filtered out by their size. The final output is shown in Fig. 3C.

In order to segment spines, the algorithm requires the computation of seed points. Using the gradient vector flow generated backbone, an inner distance map is computed. This inner distance map measures the distance of each foreground pixel to the closest central region pixel. Only pixels in the computed foreground contour are considered as possible seed points. Using the inner distance map and the ROI contours, all regional maxima are used as the seed points. These regional maxima correlate to the furthest spine pixels from the central regions of the dendrite. Each seed point is considered a possible spine detection. All contour pixels that are closer to the seed point than the closest backbone pixel are considered a part of that spine as shown in Fig. 3D. The end points of this contour are found and a line is draw to connect them. This line represents the interface or boundary between the spine and its dendrite. The contour is now filled and will be used as the final segmentation of the spine.

A. Cofilin Motility Extraction

In order to analyze the motility of cofilin, at least two adjacent frames are needed. Because individual cofilin proteins exist at the subpixel level and cannot be resolved at our (40x) magnification, they cannot be tracked individually. Since the green intensity channel tracks the fluorescence-tagged cofilin species, the intensity is directly proportional to the amount of cofilin in the pixel. While the visual changes in cofilin density are difficult to examine by eye, the system is able to estimate this information by using spatio-temporal information in the red structural channel. Using the previously segmented dendritic spines, we can approximate the amount of cofilin located in these structures. The system starts by preforming data association of segmented spines in neighboring frames to produce dendritic spine tracks. Association is chosen by largest percent of overlap with existing tracks. The ratio of overlap is sufficient as the spines are attached to a fixed location on the dendrite. Most of the dynamic motion of dendritic spines are due to sway and shape change, whereas the sway of the dendrite itself is negligible.

New tracks may be created if there is no overlap. A spine may not be detected in every frame as they may shrink into the dendrite or sway in and out of the z-axis, thereby going out of view. Because of this, a spine segmentation may be associated with any existing track as long as there is overlap with the last known location.

Because we are interested in the flow of cofilin through regions of a cell, it is useful to relate this concept to fluid dynamics. Of particular interest is the differential form of the continuity equation in fluid mechanics, which is written as:

$$\frac{\delta\rho}{\delta t} + div(f) = s, \text{ such that } f = \rho v, \quad (3)$$

where ρ is the density of the fluid particles, f is the flux of the fluid through a boundary, v is the velocity, and s is a source term. To find the change in the amount of cofilin in the spine, we want to solve for the $div(f)$ which is the "flux density" and represents the amount of flux entering or leaving a point. In florescence microscopy, fluorescence intensity levels are proportional to the amount of tagged proteins in a region. This leads to the follow proportionality formula:

$$\rho \propto \rho_i(t) = \frac{\sum_{(x,y)\in S(t)} i(x,y,t)}{A(t)}, \quad (4)$$

where $p_i(t)$ is the density of pixel intensity levels in spine $S(t)$ at time t, $i(x,y,t)$ is the intensity of pixel (x,y) and $A(t)$ is the area in pixels of spine $S(t)$. It can be assumed that cofilin neither produced nor consumed in the spine. This allows the source term s to be set to zero for all calculations of flux. Also as there is only one boundary between the spine and the dendrite, cofilin flux must be either in or out of this boundary. Solving for $div(f)$, the continuity equation becomes:

$$div(f) \propto -\frac{\delta\rho_i(t)}{\delta t}. \quad (5)$$

A comparison of cofilin flux and density can now be made by examining the intensity levels in the green cofilin channel. An increase in the average intensity in a spine represents an increase in the cofilin density of the spine and a flux of cofilin into the spine. Conversely, a decrease in the average intensity represents a decrease in cofilin density as well as a flux of cofilin out of the spine.

B. Cofilin-Spine Shape Analysis

After acquiring the flow of cofilin and the contours of dendritic spines, we relate the flow of cofilin to the shape of the spine. The first step is to classify the shape of the dendritic spine. To do this, we obtain the spine energy image representation of a spine. The binary segmentation of each spine in a track is cropped. All binary spines images are rotated so that the spine-dendrite boundary is aligned with the x-axis. In order to compute the SEI representation, these aligned cropped images are resized into 10x10 images. Given the registered binary images $B_t(x,y)$ at time t for a spine track of N frames, the spine energy image can be computed as follows:
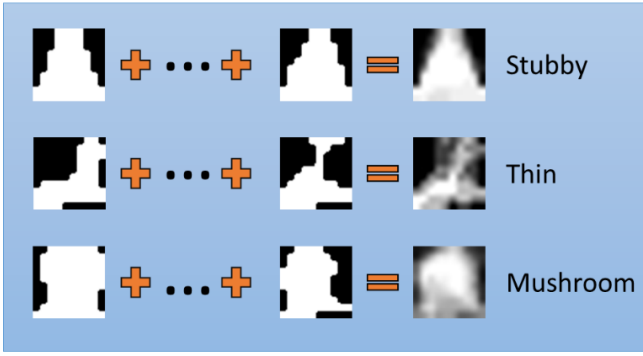
Fig. 4. Examples of aligned binary images and spine energy image for each class of dendritic spine.

$$S(x,y) = \frac{1}{N}\sum_{t=1}^{N} B_t(x,y) \qquad (6)$$

An example of the aligned binary images and SEI are show in Fig. 4.

Since the SEI images are 10x10 pixels, the dimension of the feature vector is 100, which leads to a problem with the curse of dimensionality. To account for this, principal component analysis (PCA) and multiple discriminant analysis (MDA) are used to reduce the dimensionality of the feature and find the most discriminating features for classification. PCA projects the observations to an orthogonal space that maximizes the variance in the data while minimizing the total squared error. MDA computes a function that projects the features into C-1 dimensional space that maximally discriminate between C classes. PCA is performed first and the dimensionality is reduced to the minimum number of projected dimensions with at least 90% of the variance. The project features are inputted into the MDA algorithm, producing a 2-dimensional feature space. A final classification is made with a Bayesian classifier that minimizes the expected classification cost:

$$y = \arg\min_{y=1,...,K} \sum_{k=1}^{K} P(k\,|\,x)C(y\,|\,k), \qquad (7)$$

where y is the predicted classification, K is the number of classes, $P(k|x)$ is the posterior probability of class k for observation x, and $C(y|k)$ is the cost of classifying an observation as y when its true class is k.

IV. EXPERIMENTAL RESULTS

Our data set consists of live fluorescence videos which contain 79 spines tracks recorded over approximately 30 minutes. TdTomato was used to label the entire structure of the cell (dendritic structural information) and wild type (wt)-Cofilin-GFP was used to label cofilin (cofilin distribution information). Videos varied in length from 39 to 70 frames and were collected at intervals varying from every 20 to 60 seconds. The segmentation algorithm parameters were kept constant for each video. Our system was able to find 79

properly segmented spine tracks in total. Ground truth was created by manually classifying each segmentation as stubby, thin, or mushroom. The average (mode) class type was taken as the class of the spine track.

Classification of tracks was done with 10-fold cross validation. The experiments were performed 10 times by randomly shuffling the dataset. Results are compared to a decision tree method, that uses spine height and width features. Table 1 displays the classification results. The proposed method outperforms the traditional decision tree method by close to 20%. The decision tree method was sensitive to small measurement errors at this resolution, while our proposed method is robust due to the spatio-temporal information in the spine energy images. Table 2 displays a confusion matrix of the 79 tracks.

Flux was measured for each of the 79 spine tracks. The average (mode) flux direction for each track is computed and labelled as either into the spine or out of the spine. The flux direction is sorted by class and the total count is shown in Table 3. This suggests that if the net cofilin flux remains the same in the local spine, then there will be no changes in spine structure, as seen in the stubby spines example. However, if there is a net influx of cofilin, there is a prevalence of thin, immature spines. Whereas, if there is a net outward flux of cofilin, there was a prevalence of the mature mushroom spine shapes.

V. CONCLUSIONS

In this paper, we have developed a pattern recognition system to analyze protein trafficking in neuronal florescence microscopy videos. By using spatio-temporal information, the system is able enhance low contrast/low resolution images by computing a temporal maximum intensity projection which is used to increase the signal-to-noise ratio in every frame. Also, the temporal dynamics of spines are used to generate a spine energy image which is useful in classifying different spine shapes. Lastly, we were able to estimate cofilin flux patterns and correlate them with the changing spine morphology over time. Mushroom/stubby spine shapes are recognized as mature/stable spines, whereas thin spines are classified as immature/unstable. Our data suggests that the rapid cycling of cofilin in and out of the spines leads to structural instability of the spines. This is consistent with the actin-severing/remodeling function of cofilin.

TABLE I.　　CLASSIFICATION RESULTS

DECISSION TREE	SPINE ENERGY IMAGE
$60.76 \pm 0.00\%$	$79.75 \pm 1.30\%$

TABLE II.　　CONFUSSION MATRIX

		Predicted Class		
		Stubby	Thin	Mushroom
Real Class	Stubby	40	3	2
	Thin	5	6	0
	Mushroom	4	1	18

TABLE III.　　COFILIN FLUX BY CLASS

STUBBY		THIN		MUSHROOM	
INTO	OUT OF	INTO	OUT OF	INTO	OUT OF
46.67%	53.33%	72.73%	27.27%	30.43%	69.57%

REFERENCES

[1] E. Andrianantoandro and T. D. Pollard, "Mechanism of Actin Filament Turnover by Severing and Nucleation at Different Concentrations of ADF/Cofilin," *Mol. Cell*, vol. 24, no. 1, pp. 13–23, 2006.

[2] C. Chan, C. C. Beltzner, and T. D. Pollard, "Cofilin Dissociates Arp2/3 Complex and Branches from Actin Filaments," *Curr. Biol.*, vol. 19, no. 7, pp. 537–545, 2009.

[3] A. Rao and A. M. Craig, "Signaling between the actin cytoskeleton and the postsynaptic density of dendritic spines," *Hippocampus*, vol. 10, no. 5, pp. 527–541, 2000.

[4] K. E. Sorra and K. M. Harris, "Overview on the Structure, Composition, Function, Development, and Plasticity of Hippocampal Dendritic Spines Structure of Hippocampal Dendritic Spines."

[5] H. Hering and M. Sheng, "Dendritic Spines: Structure, Dynamics and Regulation," *Nat. Rev. Neurosci.*, vol. 2, no. 12, pp. 880–888, Dec. 2001.

[6] R. Yuste and T. Bonhoeffer, "Genesis of dendritic spines: insights from ultrastructural and imaging studies," *Nat. Rev. Neurosci.*, vol. 5, no. 1, pp. 24–34, Jan. 2004.

[7] M. Matsuzaki, G. C. Ellis-Davies, T. Nemoto, Y. Miyashita, M. Iino, and H. Kasai, "Dendritic spine geometry is critical for AMPA receptor expression in hippocampal CA1 pyramidal neurons.," *Nat. Neurosci.*, vol. 4, no. 11, pp. 1086–92, Nov. 2001.

[8] I. M. Ethell and E. B. Pasquale, "Molecular mechanisms of dendritic spine development and remodeling.," *Prog. Neurobiol.*, vol. 75, no. 3, pp. 161–205, Feb. 2005.

[9] J. R. Bamburg, B. W. Bernstein, R. . Davis, K. C. Flynn, C. Goldsbury, J. R. Jensen, M. T. Maloney, I. T. Marsden, L. S. Minamide, C. W. Pak, A. E. Shaw, I. Whiteman, and O. Wiggan, "ADF/Cofilin-Actin Rods in Neurodegenerative Diseases," *Curr. Alzheimer Res.*, vol. 7, no. 3, pp. 241–250, May 2010.

[10] M. Halavi, K. A. Hamilton, R. Parekh, and G. A. Ascoli, "Digital reconstructions of neuronal morphology: three decades of research trends.," *Front. Neurosci.*, vol. 6, p. 49, 2012.

[11] M. E. Berginski, E. A. Vitriol, K. M. Hahn, and S. M. Gomez, "High-Resolution Quantification of Focal Adhesion Spatiotemporal Dynamics in Living Cells," *PLoS One*, vol. 6, no. 7, p. e22025, Jul. 2011.

[12] M. Bosch, J. Castro, T. Saneyoshi, H. Matsuno, M. Sur, and Y. Hayashi, "Structural and molecular remodeling of dendritic spine substructures during long-term potentiation.," *Neuron*, vol. 82, no. 2, pp. 444–59, Apr. 2014.

[13] I. Smal, M. Loog, W. Niessen, and E. Meijering, "Quantitative comparison of spot detection methods in fluorescence microscopy.," *IEEE Trans. Med. Imaging*, vol. 29, no. 2, pp. 282–301, Feb. 2010.

[14] T. Pecot, J. Boulanger, C. Kervrann, P. Bouthemy, and J. Salamero, "Estimation of the flow of particles within a partition of the image domain in fluorescence video-microscopy," in *2014 IEEE 11th International Symposium on Biomedical Imaging (ISBI)*, 2014, pp. 453–456.

[15] T. Pecot, C. Kervrann, J. Salamero, and J. Boulanger, "Counting-Based Particle Flux Estimation for Traffic Analysis in Live Cell Imaging," *IEEE J. Sel. Top. Signal Process.*, vol. 10, no. 1, pp. 203–216, Feb. 2016.

[16] M. Théry, V. Racine, A. Pépin, M. Piel, Y. Chen, J.-B. Sibarita, and M. Bornens, "The extracellular matrix guides the orientation of the cell division axis," *Nat. Cell Biol.*, vol. 7, no. 10, pp. 947–953, Oct. 2005.

[17] A. Rodriguez, D. B. Ehlenberger, D. L. Dickstein, P. R. Hof, and S. L. Wearne, "Automated Three-Dimensional Detection and Shape Classification of Dendritic Spines from Fluorescence Microscopy Images," *PLoS One*, vol. 3, no. 4, p. e1997, Apr. 2008.

[18] I. Y. Y. Koh, W. B. Lindquist, K. Zito, E. A. Nimchinsky, and K. Svoboda, "An Image Analysis Algorithm for Dendritic Spines," *Neural Comput.*, vol. 14, no. 6, pp. 1283–1310, Jun. 2002.

[19] C. M. Weaver, P. R. Hof, S. L. Wearne, and W. B. Lindquist, "Automated algorithms for multiscale morphometry of neuronal dendrites.," *Neural Comput.*, vol. 16, no. 7, pp. 1353–83, Jul. 2004.

[20] Y. Zhang, X. Zhou, A. Degterev, M. Lipinski, D. Adjeroh, J. Yuan, and S. T. C. Wong, "A novel tracing algorithm for high throughput imaging Screening of neuron-based assays.," *J. Neurosci. Methods*, vol. 160, no. 1, pp. 149–62, Feb. 2007.

[21] J. Cheng, X. Zhou, E. Miller, R. M. Witt, J. Zhu, B. L. Sabatini, and S. T. C. Wong, "A novel computational approach for automatic dendrite spines detection in two-photon laser scan microscopy.," *J. Neurosci. Methods*, vol. 165, no. 1, pp. 122–34, Sep. 2007.

[22] Y. Zhang, K. Chen, M. Baron, M. A. Teylan, Y. Kim, Z. Song, P. Greengard, and S. T. C. Wong, "A neurocomputational method for fully automated 3D dendritic spine detection and segmentation of medium-sized spiny neurons," *Neuroimage*, vol. 50, no. 4, pp. 1472–1484, 2010.

[23] C. Xu and J. L. Prince, "Gradient Vector Flow: A New External Force for Snakes," *IEEE Proc. Conf. Comp. Vis. Patt. Recog*, 1997.

[24] S. Basu, D. Plewczynski, S. Saha, M. Roszkowska, M. Magnowska, E. Baczynska, and J. Wlodarczyk, "2dSpAn: semiautomated 2-d segmentation, classification and analysis of hippocampal dendritic spine plasticity," *Bioinformatics*, p. 172, Apr. 2016.

[25] J. Han and B. Bhanu, "Individual Recognition Using Gait Energy Image," *IEEE Trans. Pattern Anal. Mach. Intell.*, pp. 316–322, 2006.

[26] N. Otsu, "A Threshold Selection Method from Gray-Level Histograms," vol. 9, no. 1. pp. 62–66, 1979.